Dense Microtremor observations in disaster area due to the 2016 Kumamoto Earthquake

Takao Kagawa[1], *Shohei Yoshida[1], Hiroshi Ueno[1]

1. Tottori University Graduate School of Engineering

Microtremor observations were conducted in Mashiki town and Minami-Aso village where severe damages spread over due to the 2016 Kumamoto Earthquake. Two targets are set for the observations. One is searching out the difference of ground motion between surface faulting areas without severe damage and severely damaged areas without surface faulting. Another is assessing the effect of surface geology and geographic transition on spotted damage distribution in downtown area. For the purposes, 3 components single station observations are conducted to detect predominant period at the site and array observations are made for evaluating surface velocity structures. Using the records fro microtremor observations and previously conducted aftershock observations, productive discussions about causes of disaster are expected.

Keywords: The 2016 Kumamoto Earthquake, Mashiki town, Minami-Aso village, Microtremor observation

Characterized source model for estimating strong ground motions during one of the largest foreshocks (Mw 6.0) of the 2016 Kumamoto Earthquake

*Susumu Kurahashi[1], Ken Miyakoshi[2], Kojiro Irikura[1]

1. Aichi Institute of Technology, 2. Geo-Research Institute

1. Introduction
One of the largest foreshocks (Mw 6.0) of the 2016 Kumamoto earthquake occurred along the Hinagu fault zone in Kyushu, Japan, on April 15, 2016. The maximum seismic intensity with 6 lower was observed at KMMH16 (Mashiki, epicentral distance: 11km) and KMMH14 (Toyono, epicentral distance: 8km) station. PGA of 557.9 gal is observed at the KMMH14. We estimated the characterized source model based on the slip distribution results of the waveform inversion using the strong motion data and the empirical Green's function method.
2. Source model inferred from the waveform inversion results
We analyzed the slip distribution during this earthquake using the multi-time window linear waveform inversion method (Sekiguchi et al., 2000). The data sets used for the inversion analysis were velocity waveforms of S-waves parts in the frequency range 0.1-1.0Hz at 11 stations (KiK-net, K-NET). The Green's functions were calculated using the one-dimensional velocity structure models by the discrete wavenumber method (Bouchon, 1981) with the reflection and transmission matrix method (Kennett and Kerry, 1979) at the stations. A fault plane was assumed referring to the aftershock distribution and the moment tensor solution determined by F-net.
The fault plane is divided into 81 subfaults of 1.5km×1.5km. The temporal moment release history from each subfault is modeled by a series of 4 smoothed-ramp-functions with a rise time of 0.8 second each separated by 0.4 second.
Large slip area is constructed in the proximity of the hypocenter.Seismic moment and rupture velocity are estimated 1.6×1018Nm, 2.7km/s, respectively. The synthetic waveforms at KMMH14 station fit the observed ones reasonably.

3. Characterized source model inferred from the waveform inversion results
The characterized source model is constructed based on the slip distribution from the waveform inversion. We extracted asperity from the slip distribution and high rate area (HRA) from the moment rate distribution by the criterion of Somerville et al. (1999). The area and location of the asperity and the HRA are estimated to be almost the same.
4. Estimation of strong motion generation area (SMGA) using empirical Green's function method
We analyzed the SMGA model using the empirical Green's function method. In particular, we attempted to simulate the strong ground motions at KMMH14 located near the source fault. As a result, the location of the SMGA is nearly the same as the estimated large slip area from the waveform inversion results. We obtained one of the best-fitting SMGA models choosing the starting point, rupture velocity, and rise time by comparing simulated and observed ground motions including the ground motions at KMMH14. The SMGA area and stress parameter are calculated about 33 km^2 and 7.5 MPa, respectively. The scaling relationship SMGA area versus seismic moment is consistent with on the scaling law of combined of asperities versus seismic moment by the previous study (Irikura and Miyake, 2001).
5. Conclusion
We estimated the characterized source model of the Mw 6.0 forshock of the 2016 Kumamoto earthquake

based on the slip distribution results of the waveform inversion using the strong motion data and the empirical Green’s function method. The asperity, the HRA and the SMGA of this earthquake are collocated with nearly the same area.

Acknowledgements. Seismic waveform data of the K-NET and KiK-net were used. This study was based on the 2016 research project 'Improvement for uncertainty of strong ground motion prediction' by NRA (Nuclear Regulation Authority).

Keywords: Foreshock of the 2016 Kumamoto earthquake, strong ground motion, characterized source model

Strong ground motion simulation of the main shock of the 2016 Kumamoto Earthquake using the pseudo point-source model and its improvement

*Yosuke Nagasaka[1], Atsushi Nozu[1]

1. Port and Airport Research Institute

Many near-fault strong motion records were obtained during the main shock of the Kumamoto, Japan, earthquake on April 16th, 2016. In general, observed records of such a large earthquake reflect the finiteness of the fault, that is, directivity effect. On the other hand, strong motion simulations using simple point sources and empirical site amplification and phase characteristics have well reproduced observed strong motions of large earthquakes such as the 1995 Kobe and 2011 Tohoku Great earthquakes (for example, Nozu, 2016). Investigating the applicability of the point source model to large earthquakes is important to understand the mechanism of strong motion generation. In this study, then, we constructed a pseudo point-source model (Nozu, 2012) for the main shock of the Kumamoto earthquake and the simulation results were compared with the observed records.
In the pseudo point-source model, the source spectrum is combined with the path effect, empirical site amplification factors, and empirical phase characteristics from small earthquakes to synthesize strong motions. Source parameters include the location of the point sources, corner frequencies, and seismic moments. In our model for the main shock of the 2016 Kumamoto earthquake, three subevents were placed on the fault plane along Futagawa fault: two of them were placed below Mashiki Town, about 5 km northeast from the epicenter, and the other was placed below Nishihara Village, about 15 km northeast from the epicenter. Two subevents were placed around Mashiki town to reproduce the characteristic velocity pulses and the trough in the observed Fourier spectrum at Mashiki, which was considered due to the interference of the seismic waves from two different sources. The observed and synthetic velocity waveforms (0.2-2Hz) and acceleration Fourier spectra were compared. The synthetic results generally reproduced the main features of the observed records, however, discrepancies were also observed. One of them is the underestimation in the frequency range below 0.6 Hz, which was considered due to the contribution from shallow slip including near-field and intermediate-field terms, because the effect of shallow slip were not considered in the point source models. Large permanent displacements could be due to the near-field and intermediate-field terms. We need to incorporate the effect of shallow slip including these terms if they contribute to near-fault ground motions around 0.6 Hz, because ground motions in this frequency range contribute to damage to structures. Another discrepancy found in the point-source model is the underestimation at the stations northeast of the epicenter, around Aso Caldera. This is presumably due to the fact that the point source models cannot capture the directivity effect, whereas the actual rupture proceeded northeast and caused significant forward directivity effect at stations located northeast of the fault.
We need to model not only the deep subevents but also the shallow slip in order to adequately conduct strong motion simulation for the 2016 Kumamoto earthquake. We will use an ordinary point source model for the deeper part, and incorporate the effect of shallow slip including near and intermediate-field terms. The original model was intended to explain whole strong motions without considering the shallow slip. In the new model, by incorporating the effect of the shallow slip, the parameters for the deeper point source will also be affected. The new model will be presented in the meeting.

Keywords: The 2016 Kumamoto earthquake, strong ground motion simulation, pseudo point-source model

Estimation of characterized source model of the mainshock in the 2016 Kumamoto earthquakes using the stochastic Green's function method

*Atsuko Oana[1], Kazuo Dan[2], Junichi Miyakoshi[2], Hiroyuki Fujiwara[3], Nobuyuki Morikawa[3], Takahiro Maeda[3]

1. Shimizu Corporation, 2. Ohsaki Research Institute, 3. National Research Institute for Earth Science and Disaster Resilience

We estimated a characterized source model for the mainshock in the 2016 Kumamoto earthquakes using the stochastic Green's function method, in preparation for strong motion prediction at points where no observation records were obtained.
Records of the seven KiK-net observation stations, including KMMH16 (Mashiki), were targets of this study. First, the strong motions on the engineering bedrock were estimated in order to remove the site effects of the shallow soil from the observation records. In concrete, the soil models were identified so that the transfer functions between the surface records and the borehole records could be reproduced for less 5 Hz. Then, the strong motions on the engineering bedrock were calculated by the multiple reflection theory using the identified soil models and the borehole records. The NS and EW components were calculated separately, because it was difficult to invert both of them back to the motions on the engineering bedrock using the common identical soil model.
Next, one-dimensional velocity structure models from the seismic bedrock to the engineering bedrock were assumed based on the Japan integrated velocity structure model (Koketsu et al., 2012), then those models were adjusted so that the dominant frequencies of the models corresponded to those of the H/V spectral ratios of the small aftershock records.
The stochastic Green's functions were generated using the stochastic amplitude model and the envelope function model (Boore, 1983), especially for the area close to the fault. Then, the waves that had bell-shape forms were selected based on Kagawa (2004). The cutoff frequency f_{max} was assumed to be 4 Hz. The Q-value was $62f^{0.87}$ (for f less than 1 Hz) taken from Satoh (2016). The source model was assumed as an SMGA (Strong Motion Generation Areas) model. The location and area of SMGA were set by trial and error, inside the region of the source inversion of Asano and Iwata (2016). The slip of each SMGA was determined with reference to the slip distribution of source inversion (e.g., Asano and Iwata, 2016; Hikima, 2016), and at the same time, so that the displacements and the velocity response spectra in long period range of our simulation agreed with the observed ones. The stress drop of each SMGA was determined so that the accelerations, velocities, and velocity response spectra in short period range of our simulation agreed with the observed ones. The location of the rupture initiation point of Hinagu fault was the same as that by JMA (2016), and that of Futagawa fault was slightly deeper than Hinagu one and located at the southern edge of the fault. The rupture velocity of the small SMGA in Futagawa fault was 2.7 km/s, and that of the large SMGA in Futagawa fault and that of Hinagu fault were 3 km/s.
The obtained source model had a short-period level of 1.14×10^{19} Nm/s^2, which was smaller than Satoh (2016) and Irikura et al. (2017) and larger than Nakano and Kawase (2016). Furthermore, the short-period level was smaller than the empirical relationship between the seismic moment and short-period level of crustal earthquakes proposed by Dan et al. (2001), and was slightly smaller than the empirical relationship of crustal earthquakes caused by strike-slip faults proposed by Dan et al. (2011). The averaged response spectral ratio between the observation records and the simulation results became almost 1 in the period range of 0.2-5 s. However, the ratio was smaller than 1 in the period range longer

than 5 s. This is because the seismic moment of the obtained SMGA model was about 60 % of that of the whole fault (e.g., F-net, 2016). While the duration of simulation results in the area close to the fault trace corresponded well to the observed ones, those of the simulation results in the area far from the fault trace were shorter than the observed ones. This attributes to a problem for setting the amplitude and the envelope function of the Green’ s function in the area far from the fault trace.

Keywords: 2016 Kumamoto earthquake, Stochastic Green’ s function method, Characterized source model

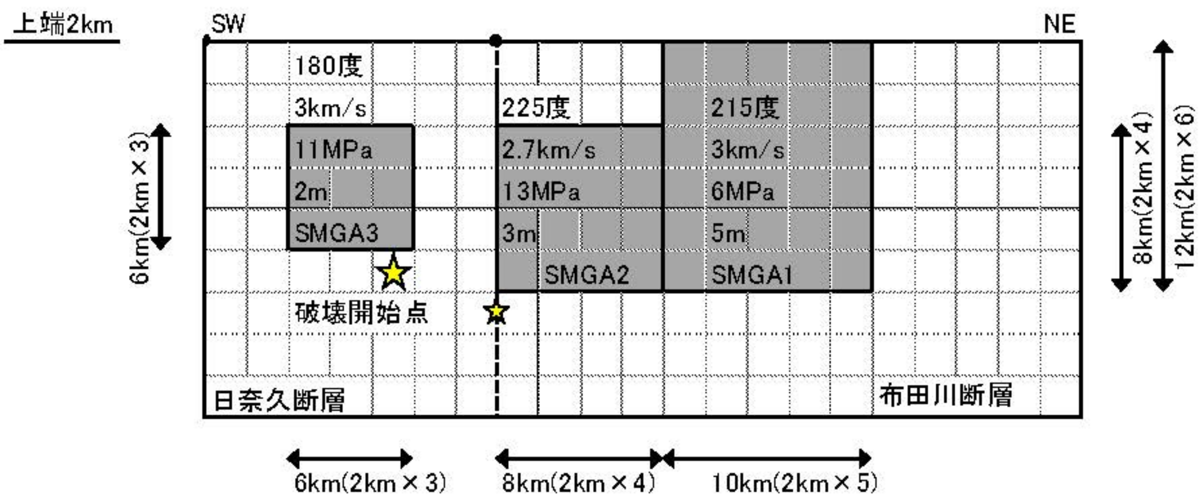

（数値：すべり角[度]、破壊伝播速度[km/s]、応力降下量[MPa]、すべり量[m]）

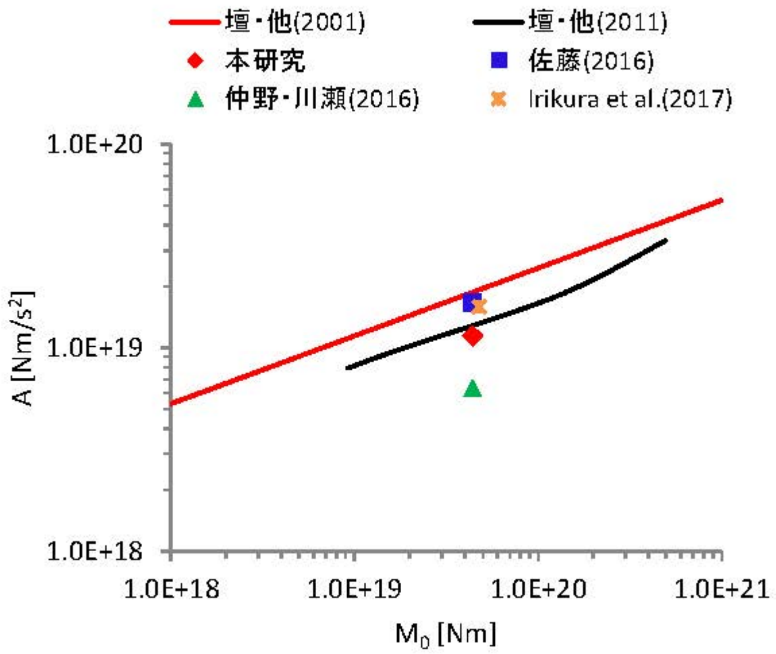

※本研究、佐藤(2016)、仲野・川瀬(2016)の地震モーメント M_0 は F-net の 4.42×10^{19} Nm とした。佐藤(2016)と Irikura et al. (2017)の短周期レベル A は、SMGA の応力降下量と面積を用いて算出した。

Source model and strong ground motion simulation for the 2016 Mid Tottori prefecture, Japan, earthquake (M_w6.2) based on the empirical Green’s function method

*Kazuhiro Somei[1], Takaaki Ikeda[2], Toshimitsu Nishimura[1], Ken Miyakoshi[1]

1. Geo-Research Institute, 2. Nagaoka University of Technology

At 14:07 Japan Standard Time (JST=UT+9) on October 21, 2016, an inland crustal earthquake (M_{JMA}6.6, M_w6.2) with strike-slip occurred in the mid Tottori prefecture, Japan. Strong ground motions with a peak acceleration 1381 cm/s^2 were recorded at one of the nearest strong motion stations, TTR005, about 10 km away from the hypocenter. For understanding the physical mechanisms of strong motion generation processes during this event, we estimate the source model composed of strong motion generation areas (SMGA) to explain the observed strong motion records in broadband frequency range between 0.3 and 10 Hz.
In this study, we use the empirical Green’s function method to simulate the broadband strong motion records at 18 sites of K-NET and KiK-net located around the source region. The observed ground motion records of M_w4.1 event (element event) occurring at 12:12 on October 21, 2016, are used as the empirical Green’s functions. For an objective estimation of corner frequencies for the target and element events, we apply the source spectral ratio fitting method (Miyake et al., 1999). From the obtained corner frequencies, scaling parameters *N* and *C*, which required for the empirical Green’s function method of Irikura (1986), are determined. Then, the parameters of each SMGA (e.g., the size, rupture starting point, rise time, rupture velocity, and relative location from the hypocenter) are estimated by trial and error method. Since we can clearly see the S-wave portion consists mainly of two wave packets for observed waveform at TTR005, we assume two squared SMGAs on the fault plane, and will call the SMGA that generates the first S-wave packet SMGA1 and that generating the second SMGA2.
As a result, we construct the source model with SMGA1 located including the hypocenter and SMGA2 located north from the hypocenter. The sizes of SMGA1 and 2 are 30.3 and 19.4 km^2, respectively. The stress drops of both SMGAs are estimated to be same as 16.6 MPa. Rupture propagations within SMGAs bring forward and backward rupture directivity effect in ground motion observed at TTR005 that is located near-source fault: The forward directivity effect by SMGA1 contributes to the pulse-shape wave packet for fault-normal component observed at TTR005. On the other hand, the random-shape wave packet is generated by the backward directivity effect from SMGA2. However, the amplitude of pulse-shape wave from SMGA1 is not as large as that expected from the ground motion prediction equation (GMPE), because the rupture within SMGA1 propagates bilaterally from the center of SMGA1 to both north and south directions. For other sites located around the source region, the SMGA1 mainly reproduces the observed acceleration, velocity, and displacement waveforms fairly well. Thus, the near-source strong ground motion observed at TTR005 gives us the insight into the possiblity for the presence of SMGA2. In order to improve the reproducibility of observed ground motions, the parameters of SMGAs need to be examined objectively in more detail.

Acknowledgements: We use the hypocentral information catalog of JMA, the moment tensor catalog by F-net, and the strong motion data from K-NET, KiK-net, and F-net provided by NIED.

Keywords: The 2016 Mid Tottori prefecture earthquake, Strong motion generation area, Empirical Green’s function method

A heterogeneous SMGA model for plate boundary earthquakes

*Haruko Sekiguchi[1], Kimiyuki Asano[1], Tomotaka Iwata[1]

1. DPRI, Kyoto University

Seismic waves in the frequency range 0.1–10 Hz are mainly radiated from strong motion generation areas on a source fault. A heterogeneous SMGA (Strong Motion Generation Area) model was constructed inspired by the area-stress drop relationship of SMGAs of plate boundary earthquakes. The relationship shows large scatter of average stress drop for small SMGAs and small scatter for large SMGAs. The relationship was well modeled by adopting k^{-1} spatial spectrum and lognormal probability distribution for the stress drop distribution, and tuning the parameters of those distributions. This model may make it possible to predict the strong short-period pulse amongst the SMGA pulse, which has been indicated by forward waveform modeling in previous studies (e.g., Matsushima and Kawase, 2006; Nozu 2012; Kurahashi and Irikura, 2013).

Keywords: Strong motion generation area, heterogenous source, stress drop

Parameter Study on Near Fault Strong Ground Motion Considering Randomness of Faulting Process

*Junpei Kaneda[1], Yoshiaki Hisada[1]

1. Kogakuin University

During the 2016 Kumamoto earthquake, the near fault strong ground motions in Mashiki City showed that the EW components (closet to the fault normal direction) were dominant over the NS components. This was probably caused by the combined effects of the upward directivity pulse (e.g., Miyatake (2016)) and the fling step (e.g., Hisada et.al. (2016)). On the other hand, the near fault strong ground motion in Nishihara Village also showed the dominant EW components, which was caused by the fling step, but did not showed the forward directivity pulse. This may be caused by the complex faulting process, and/or the complex underground structures, which prevents the generation of directivity pulses (e.g., Hisada et.al. (2016)). In order to confirm these phenomena, we carried out the parameter studies based on the recipe for strong motion prediction method. We will present the detail results on the conference.

Keywords: Near Fault Strong Ground Motion, Directivity Pulse, Randomness of Faulting Process

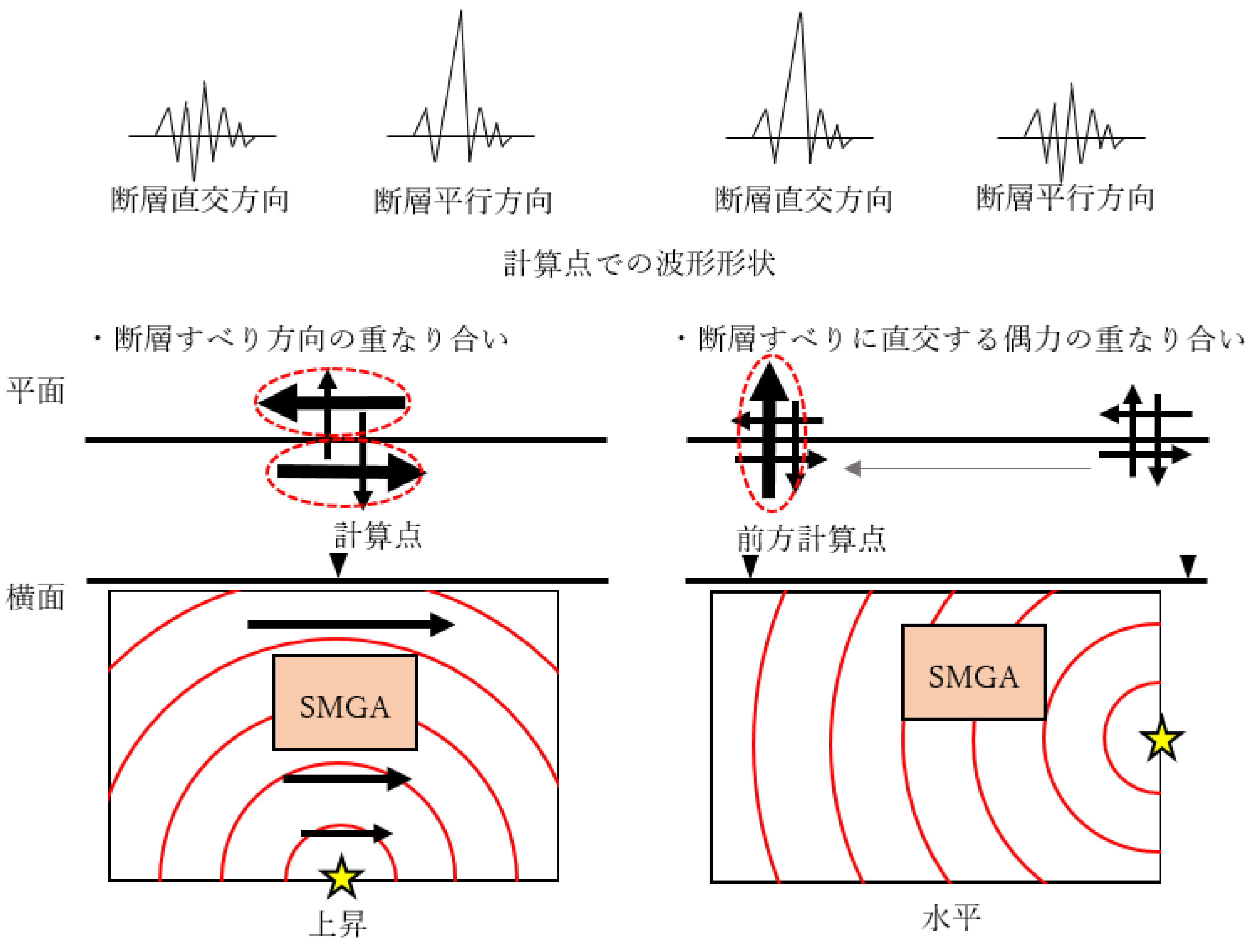

図 1 伝播特性と指向性パルス発生の概念図(宮武(2016)を参照)

Site response of vertical component ground motion excited by obliquely incident S wave

*Kunikazu Yoshida[1], Ken Miyakoshi[1]

1. Geo-Research Institute

We investigate vertical ground motion of S-wave portion in a continuous velocity structure model. In many case, vertical ground motions of S-wave part have been assumed as a wavefield of that part is dominated by P wave. However, this assumption sometimes seems to be inappropriate to real data. We calculated spectral ratios of surface to borehole ground motions on P and S wave parts recorded at 6 KiK-net vertical array sites. At some sites (e.g., KMMH16), the spectral ratios on P and S wave parts have similar shapes, however, some other sites (e.g., TYMH02) indicated different shapes of spectral ratio between P and S wave parts. The site which have different spectral ratios between P and S wave are expected that seismic velocities in the sediments (between the Earth surface and seismic bedrock) below the sites are continuously varied with depth, and have not clear discontinuity. Theoretical examination of vertical component ground motions excited by the obliquely incident S-wave pulse (incident angle=10°) indicate that a spectral ratio of surface and borehole data in a continuous velocity model (mirage model) differs from one in a discontinuous velocity model (contrast model) (Fig. A). Difference of the spectral ratio in the contrast model between for the oblique incident S-wave and for the vertical incident P-wave indicates that the assumption of the P-wave incident in the previous studies is not reasonable for the continuous velocity structure. We examined vertical component ground motion recorded at TYMH02 KiK-net vertical array assuming a continuous velocity structure model. Although the synthetic waveforms at the surface from the borehole for the vertical incident P-wave indicated unacceptable monotonic waveforms, the synthetics for obliquely incident S-wave were comparable to the observed one (Fig. B).
Acknowledgement: KiK-net data was used.

Keywords: continuous velocity structure, oblique incident, S wave, vertical component

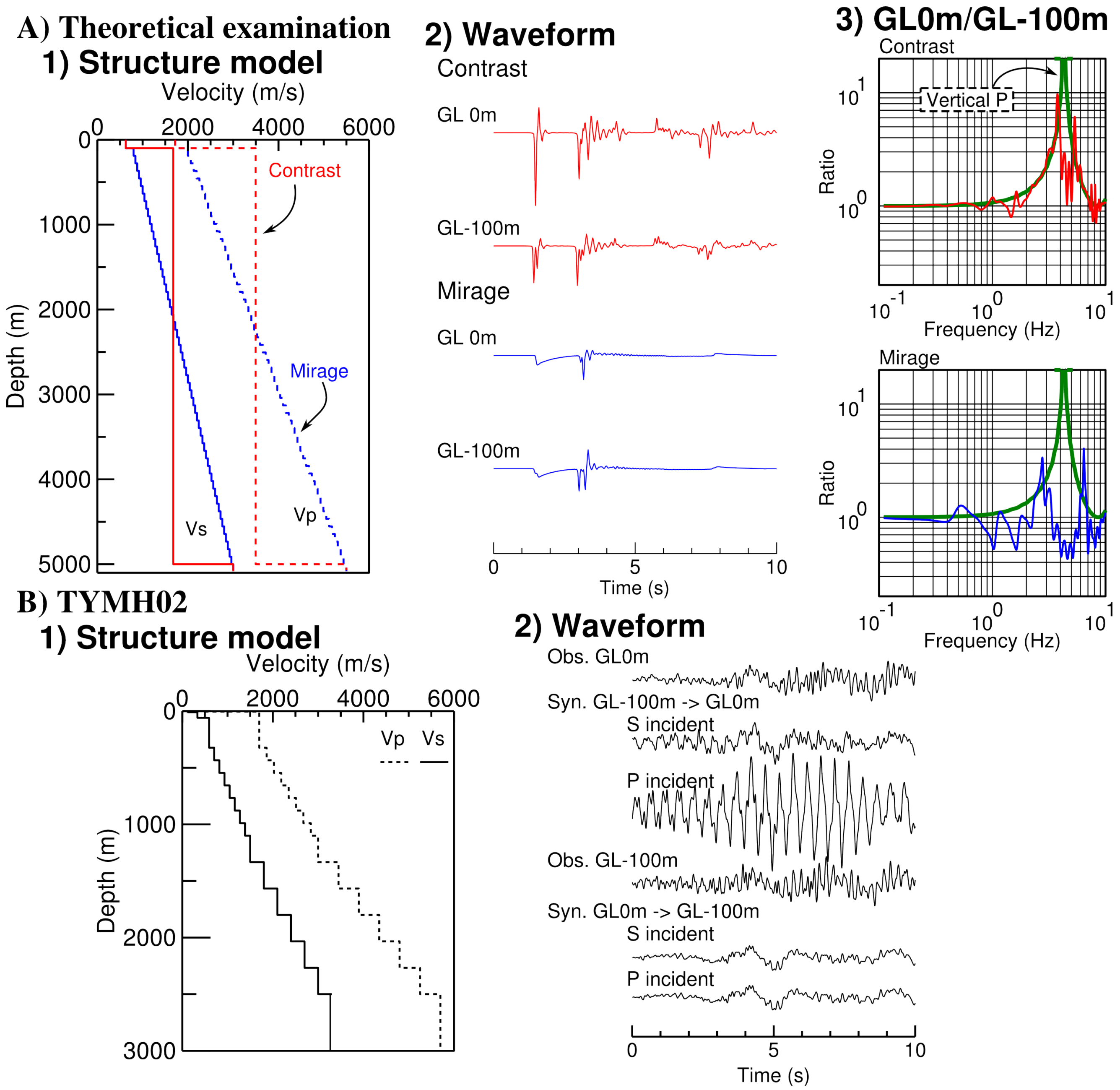
A) Theoretical examination
1) Structure model
Velocity (m/s)
0
2000
4000
6000
Depth (m)
1000
2000
3000
4000
5000
Contrast
Mirage
Vs
Vp
2) Waveform
Contrast
GL 0m
GL-100m
Mirage
GL 0m
GL-100m
Time (s)
5
10
3) GL0m/GL-100m
Contrast
Vertical P
Ratio
Frequency (Hz)
Mirage
B) TYMH02
1) Structure model
Velocity (m/s)
Vp
Vs
Depth (m)
2) Waveform
Obs. GL0m
Syn. GL-100m -> GL0m
S incident
P incident
Obs. GL-100m
Syn. GL0m -> GL-100m
S incident
P incident
Time (s)

Strong Ground Motion along the Joetsu Shinkansen during the 2004 Chuetsu Earthquake and Aftershock Sequence

*Yifei Chen[1], Hiroe Miyake[2]

1. GSII, The University of Tokyo, 2. III, The University of Tokyo

During the 2004 Chuetsu earthquake occurred at 17:56 on 23 October 2004, many relatively large-magnitude aftershocks occurred following the main shock (Mw 6.6). In the main shock, the seismic intensity meter of Kawaguchi-cho in Niigata prefecture recorded seismic intensity level 7, and equivalent seismic intensity level 7 was observed at K-NET Ojiya of NIED and Shinkawaguchi electrical substation of JR East (ARAIC, 2007). There were more than 10 earthquakes observed whose seismic intensity level were larger than 5+. All of them were observed in the areas such as Ojiya, Nagaoka, and Uonuma of Niigata prefecture. Large seismic intensity was observed in the watershed of the Shinano river where was near the epicenter and has a complex velocity structure with large site amplification factors.

During the 2004 Chuetsu earthquake, the first derailment of Shinkansen under operation ever occurred in which was slight south of the Nagaoka station of the Joetsu Shinkansen. The strong motion along the Joetsu Shinkansen has been discussed by Mori and Kazuni (2005), Nakamura (2006), and ARAIC (2007). Mori and Kazuni (2005) pointed out the influence of strong motion whose period was less than 0.5 second. On the other hand, the predominant period of the observed strong motion ranged from Ojiya to Nagaoka during the 2004 Chuetsu earthquake was 1 second. The 2004 Chuetsu earthquake and its aftershocks occurred in conjugated fault plane systems, both the hypocenter and velocity structures of which were complex. For that reason, it is difficult to obtain ground motion simulation results which are consistent with observation records. In this research, we focus on the arrival times of P-wave and S-wave for the 2004 Chuetsu earthquake and the importance of the distribution of strong ground motions. We also discuss the distribution of strong motion in the 2004 Chuetsu earthquake along the Joetsu Shinkansen by conducting ground motion simulation of aftershocks whose point-source assumption are easy to assume.

In the analysis, we deal with seismic intensity meters such as Niigata prefecture, JMA, K-NET, and KiK-net, using earthquake source models from F-net and Hikima and Koketsu (2005). We use J-SHIS as the initial velocity structure model. We also conduct ground motion simulation by using 3-D finite difference method from Aoi and Fujiwara (1999) in a period rang longer than 2 second and the stochastic Green’s function method by Dan and Sato (1998) in a period range shorter than 2 second. Calculation results are compared with the ground motion prediction equation of Si and Midorikawa (1999).

Keywords: 2004 Chuetsu earthquake, Joetsu Shinkansen, strong motion data, strong motion simulation

ERI Strong Motion Observation Network and Database

*Hiroe Miyake[1], Kazuki Koketsu[1], Takashi Furumura[1], Koji Miyakawa[1], Shinichi S Tanaka[1]

1. Earthquake Research Institute, University of Tokyo

Earthquake Research Institute, University of Tokyo (ERI) has performed strong motion observation since 1953, then currently operates the strong motion network with 64 stations. Most stations are located on the ground surface with K-NET95, and several stations with JEP-4B3 & SMAC-MDU or JEP-4B3 & AJE8200 are installed both at the borehole and the ground surface for better understanding of site response. Recently, we upgrade several stations in the rock tunnels and start continuous observation with JEP-8A3 & HKS9700 that can record distant earthquakes even occurred in the southern hemisphere. The data are transmitted to ERI every second via JDXnet by the mobile router for cell phones.

In addition to the Izu & Suruga bay, Ashigara valley, and southern Kanto regions, recently most offline stations are installed in the Nagano and Suwa basins as a framework of joint strong motion observation with Shinshu University. These stations are nearby the active fault traces such as the Itoigawa-Shizuoka tectonic line. The dominant periods of the Ashigara valley and the Suwa basin range between 1 to 3 s, that may affect largely on seismic intensity measures. The stations succeeded to record the 2009 Suruga-bay intraslab earthquake and the 2011 Tohoku megathrust earthquake. Strong azimuth variation along the coast line of the Suruga bay were captured during the 2009 Suguba bay earthquake, and significant local amplification in a period range of 2 to 3 s were seen in the Ashigara valley, rather than the Kanto basin during the 2011 Tohoku earthquake.

ERI established strong motion observation database in 2008. The data are open to the public via http://smsd.eri.u-tokyo.ac.jp/smad/ with K-NET format. Data of temporary strong motion observation by portable sensors after the 2004 Chuetsu, 2005 Fukuoka, 2007 Chuetsu-oki, and 2008 Iwate-Miyagi earthquakes are also open on the website with publications.

Keywords: strong ground observation network, database, temporary strong motion observation, joint strong motion observation, continuous observation